

First observation of cyclotron radiation from MeV-scale e^\pm following nuclear β decay

W. Byron,^{1,2} H. Harrington,^{1,2} R. J. Taylor,^{3,4} W. DeGraw,^{1,2} N. Buzinsky,^{1,2} B. Dodson,^{1,2}
 M. Fertl,⁵ A. García,^{1,2} G. Garvey,^{1,2} B. Graner,^{1,2} M. Guigue,⁶ L. Hayen,^{3,4} X. Huyan,⁶
 K.S. Khaw,^{1,2} K. Knutsen,^{1,2} D. McClain,^{7,8} D. Melconian,^{7,8} P. Müller,⁹ E. Novitski,^{1,2} N. S. Oblath,⁶
 R. G. H. Robertson,^{1,2} G. Rybka,^{1,2} G. Savard,⁹ E. Smith,^{1,2} D.D. Stancil,¹⁰ M. Sternberg,^{1,2} D. W. Storm,^{1,2}
 H. E. Swanson,^{1,2} J. R. Tedeschi,⁶ B. A. VanDevender,^{6,1} F. E. Wietfeldt,¹¹ A. R. Young,^{3,4} and X. Zhu^{1,2}
 (He6-CRES collaboration)

¹*Department of Physics, University of Washington, Seattle, WA 98195*

²*Center for Nuclear Physics and Astrophysics, University of Washington, Seattle, WA 98195*

³*Physics Department, North Carolina State University, Raleigh, NC 27695*

⁴*The Triangle Universities Nuclear Laboratory, Durham, NC 27708*

⁵*Institute for Physics, Johannes-Gutenberg University Mainz, 55128 Mainz, Germany*

⁶*Pacific Northwest National Laboratory, Richland, WA 99352*

⁷*Department of Physics & Astronomy, Texas A&M University, College Station, TX 77843*

⁸*Cyclotron Institute, Texas A&M University, College Station, TX 77843*

⁹*Physics Division, Argonne National Laboratory, 9700 S. Cass Ave., Argonne, IL 60439*

¹⁰*Department of Electrical and Computer Engineering,*

North Carolina State University, Raleigh, NC 27695

¹¹*Department of Physics and Engineering Physics, Tulane University, New Orleans, LA 70118*

(Dated: September 8, 2022)

We present an apparatus for detection of cyclotron radiation that allows a frequency-based β^\pm energy determination in the 5 keV to 5 MeV range, characteristic of nuclear β decays. The cyclotron frequency of the radiating β particles in a magnetic field is used to determine the β energy precisely.

Our work establishes the foundation to apply the cyclotron radiation emission spectroscopy (CRES) technique, developed by the Project 8 collaboration, far beyond the 18-keV tritium endpoint region. We report initial measurements of β^- s from ${}^6\text{He}$ and β^+ s from ${}^{19}\text{Ne}$ decays to demonstrate the broadband response of our detection system and assess potential systematic uncertainties for β spectroscopy over the full (MeV) energy range. This work is an important benchmark for the practical application of the CRES technique to a variety of nuclei, in particular, opening its reach to searches for evidence of new physics beyond the TeV scale via precision beta-decay measurements.

Precision measurements of low-energy observables probe the existence of exotic interactions at very high energy scales through forces mediated by the exchange of virtual particles with very large masses. β spectroscopy, in particular, has received renewed interest due to its intrinsic sensitivity to chirality-flipping interactions in the electroweak sector [1, 2]. Crucially, distortions to the β spectrum depend linearly on exotic couplings via a characteristic Fierz interference term. Measurements of the Fierz parameter, b_{Fierz} , at the part-per-thousand level probe new physics at $\mathcal{O}(10 \text{ TeV})$ [3–5]. Experiments using traditional detector technology have demonstrated percent-level precision [6, 7], with a number of ongoing efforts [8–13] aimed at improving control over inescapable systematic effects such as β (back-)scattering and bremsstrahlung losses. Novel technologies such as neutral atom and ion traps have been employed to reduce these effects, some reaching 0.3% precision in parameters of the angular distribution [14–17]. Alternative technologies such as superconducting spectrometers [18] and new ion traps [19, 20] are being developed and have shown the potential for similar precision capabilities [21, 22].

Here, we present the first detection of MeV-scale β^\pm particles following the decays of ${}^6\text{He}$ (β^- endpoint $\approx 3508 \text{ keV}$) and ${}^{19}\text{Ne}$ (β^+ endpoint $\approx 2216 \text{ keV}$) extending a technique developed by the Project 8 collabora-

tion called Cyclotron Radiation Emission Spectroscopy (CRES) [23–25], far beyond the 18-keV tritium endpoint region. Both ${}^6\text{He}$ and ${}^{19}\text{Ne}$ decay almost exclusively to the ground state of their progeny, have considerably simplified nuclear structure corrections due to an underlying isospin symmetry, and have a precise theoretical characterization of their decay properties [26–29]. Interestingly, a measurement of the ratio of β energy spectra of these isotopes presents an enhancement in sensitivity to a possible Fierz term since the sign of b_{Fierz} is opposite in the two cases [30] while eliminating many systematic effects arising from common spectral distortion.

As first demonstrated by the Project 8 collaboration [24], one can perform β spectroscopy by measuring the frequency of the cyclotron radiation of an electron in a magnetic field,

$$f = \frac{|e|c^2 B}{2\pi E}, \quad (1)$$

with e and E the electron charge and total energy, and B the magnitude of the field. Using a waveguide the $\mathcal{O}(\text{fW})$ radiation can be detected. Unlike Project 8, where sensitivity is required for mildly-relativistic electrons near the tritium endpoint, we demonstrate CRES across a wide energy range. This was achieved via a broader RF band and by scanning the magnetic field.

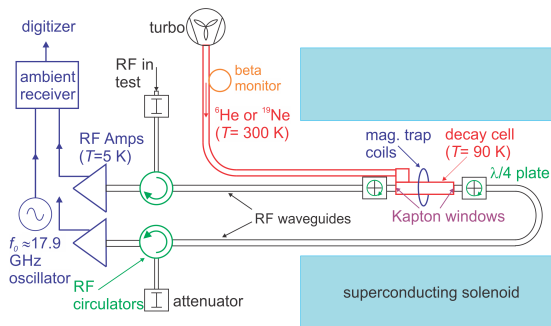


FIG. 1. He6-CRES RF setup. The radioactivity is compressed by a turbo pump into a decay cell with Kapton windows. The decay cell ($T \approx 90$ K to allow for calibrations with $^{83\text{m}}\text{Kr}$) is part of an RF waveguide system that transports signals to two low-noise amplifiers ($T \approx 5$ K).

Unlike traditional spectroscopy technology using semiconductor or scintillator detectors, the CRES technique does not rely on β energy loss in matter, obviating percent-level corrections due to β (back-)scattering and bremsstrahlung losses. The β energy is determined from the observed frequency of the cyclotron radiation and the magnitude of the magnetic field, both of which can be determined very precisely. This allows measurement of the β energy with better than part-per-thousand precision. Finally, backgrounds are strongly suppressed, because β s which are not magnetically trapped reside in the observation period for less than a nanosecond, and β s emitted from the guide wall do not contribute to signals since their helical motion results in them returning to the wall and disappearing within nanoseconds.

The radioactivity is produced by beams from the FN-tandem accelerator at the University of Washington: via $^7\text{Li}(d, ^3\text{He})^6\text{He}$ bombarding a molten lithium target with an 17.8-MeV deuteron beam [31] and via $^{19}\text{F}(p, n)^{19}\text{Ne}$ on an SF_6 gaseous target with a 12-MeV proton beam, similar to the Berkeley-Princeton source [32–35]. The radioactivity is transported to a low-background room through a 15-cm-diameter, 8-m-long stainless-steel pipe, at the end of which a turbo pump is used to compress it into the decay cell, as sketched in Fig. 1. Calibrations were performed with a $^{83\text{m}}\text{Kr}$ source, produced from ^{83}Rb embedded in zeolites [36] and connected to the apparatus.

A magnet with maximum field of 7 T and uniformity of a few parts per million per cm is used to provide the main field, and a system of three additional non-superconducting coils is used to provide a magnetic trap with fields typically of one part per thousand of the main field. Figure 2 shows the trapping-coils field.

Figure 3 sketches how different parts of the β spectrum of ^{19}Ne are covered by our bandwidth. Measurements taken at each field are normalized by total number of decays, N_{tot} , in order to assemble them into a full spectrum. N_{tot} is determined by a β monitor, shown in Fig. 1: a 3.8-cm-diameter port with a 1/8-mm thick Cu foil allows β s to be observed by a 5-mm-thick scintillator coupled

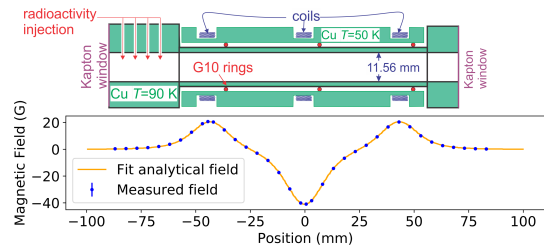


FIG. 2. Top: decay cell geometry with trap coils. Bottom: field profile from trap coils used for magnetic trapping of β s.

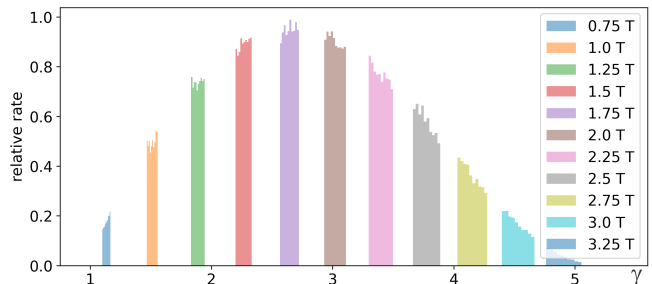


FIG. 3. Simulations (each 10^4 counts) of the ^{19}Ne β spectrum versus $\gamma = E/mc^2$ demonstrating our RF coverage. For clarity, only simulations for integer multiples of 0.25 T are shown.

to 4 SiPM readouts. The density of radioactivity in the vacuum side of this port is in dynamical equilibrium with that in the decay cell.

The circularly-polarized RF radiation produced in the decay cell (itself a 11.56-mm diameter circular waveguide) is converted into linearly polarized microwaves by $\lambda/4$ phase-retarding polarizers and transported via WR-42 rectangular waveguides to low-noise amplifiers (LNAs). The LNAs [37] are kept at ≈ 5 K and the RF noise is ≈ 60 K, dominated by the coupling of the 90-K thermal noise in the guide. Signals from the LNAs are mixed with a 17.9 GHz reference oscillator in a heterodyne receiver at ambient temperature, reducing signal frequencies from 18–19.1 GHz down to 0.1–1.2 GHz. This is a much broader bandwidth than the three 100-MHz-bandwidth channels needed for the tritium spectrum [38]. A ROACH2 system [39] digitizes the time-series signals at 2.4 GHz in $\approx 50\mu\text{s}$ segments and converts them by fast Fourier transform (FFT) for storage to disk typically at $\approx 600\text{MB/s}$.

FFT data are sequentially arranged as ‘slices’ of power versus frequency on spectrograms. Figure 4 shows data taken with the $^{83\text{m}}\text{Kr}$ source. Charged particles create tracks in the spectrogram. The slow increase of frequency versus time is due to energy radiated by the particle. The sudden jumps are due to scattering off residual atoms. The pressure in the decay cell, achieved via getter and cryo pumps, was $\approx 10^{-7}$ Torr, and dominated by residual hydrogen, nitrogen, and water. To interpret the spectrograms the C++ package Katydid [40], adapted from

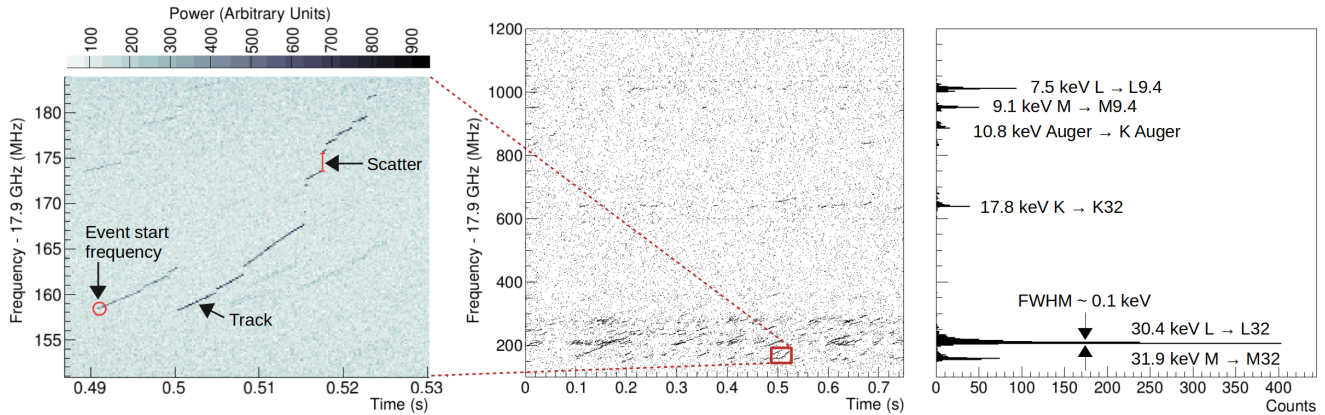


FIG. 4. $^{83\text{m}}\text{Kr}$ data taken with $B = 0.68$ T. Center: full bandwidth *sparse* spectrogram showing dots for every point with $\text{SNR} > 6$, demonstrating the bandwidth (1.1 GHz) capability. Left: zoomed-in section exemplifying an event composed of multiple tracks. Right: histogram obtained after track identification, showing simultaneous observation of the 7–32 keV lines.

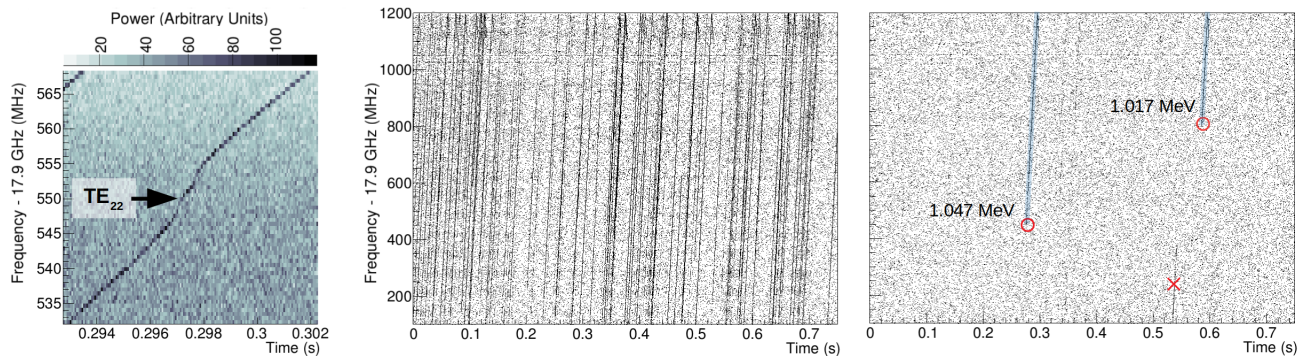


FIG. 5. CRES events from ^{19}Ne and ^6He . Left: zoomed-in section of a spectrogram showing slope variations due to coupling to higher modes. Center: sparse spectrogram of electron tracks from ^6He decay taken at $B = 2$ T using a static magnetic trap, showing the high density of tracks. Right: positron tracks from ^{19}Ne at $B = 2$ T, but with the magnetic trap on cycles of 50 ms on–50 ms off, simplifying track identification. Tracks starting within the observation band are shown with red circles and another, starting at lower frequencies and rejected, is indicated with a red cross. Kinetic energies are indicated in MeV and known to better than a part per thousand.

Project 8, is used to determine initial β energies and create histograms, as shown in Fig. 4.

The bandwidth was selected to measure only in the $\text{TE}_{1,1}$ mode, with cutoff at 15.2 GHz. The next mode, $\text{TM}_{0,1}$, has a cutoff at 19.9 GHz. The track slope, df/dt , is a proxy for the β 's radiated power. We found significant deviations from the slopes expected assuming coupling only to the $\text{TE}_{1,1}$ mode. The radiated power in a waveguide differs significantly from the relativistic Larmor formula [41]. In a waveguide, the time dependence of the wave amplitude for a mode is given by [41, 42]:

$$A_{n,m}(t) \propto \int d^3x \mathbf{J}(\mathbf{r}, t) \cdot \mathbf{E}_{n,m}(\mathbf{r}) \quad (2)$$

where $\mathbf{J}(\mathbf{r}, t)$ is the current density generated by the moving β and $\mathbf{E}_{n,m}$ represents the mode electric field. Due to the inhomogeneous fields of guide modes, the current couples to the fundamental and higher harmonic frequencies. The higher harmonics of the coupling to the $\text{TE}_{1,1}$

mode are small, but the complex structure of other modes leads to some higher harmonics coupling strongly, especially for non-concentric trajectories. The power radiated into a given mode peaks at the cutoff frequency [43]. For example, the $\text{TE}_{2,2}$ mode cutoff is 55.36 GHz which corresponds to the third harmonic of a β gyrating at 18.45 GHz (well within our bandwidth). We observed increased slopes at 18.45 GHz, in agreement with this expectation. Figure 5 shows ^{19}Ne and ^6He spectrograms.

Event analysis involves (1) applying a signal-to-noise cut, (2) identifying all tracks associated with a single decay event and (3) ensuring the beginning of an event occurs during the observation window. Events which satisfy these conditions contribute to the reconstructed β spectrum.

While the time interval between scatters for the low-energy electrons from $^{83\text{m}}\text{Kr}$ in Fig. 4 is ≈ 5 ms, it extends by more than a factor of 20 for the higher-energy β s of Fig. 5. This is due to the decrease in the scattering

cross section for β s on residual gas atoms as the β energy increases. Longer tracks make identifying the beginning of an event easier, since scattering can lead to misidentifying the initial frequency. However, this implies that particles can accumulate in the trap, resulting in multiple tracks in a given spectrogram, associated with different decay events.

The accumulation of trapped particles is controlled by periodically switching the trapping coils on and off for 50 ms. A higher duty cycle is preferable, but not currently viable due to eddy currents in the decay cell. We plan to reduce the trap-off time to below 1 ms with a redesigned decay cell to reduce field diffusion times. Figure 5 (right panel) shows that trap cycling effectively empties the trap, yielding a manageable track density. Despite the success of trap cycling, there remains a potential source of spectral distortions: events that correspond to initial frequencies lower than the observational window can be misidentified as events starting at the lowest observing frequency. Using a buffer region for vetoing such events solves the issue. Figure 5 (right panel) also shows that tracks that started at frequencies below the observational window were successfully rejected as candidate events.

An additional difference observed between the tracks for high-energy β s compared to those from $^{83\text{m}}\text{Kr}$ is that the slopes are a factor up to two orders of magnitude larger. Figure 6 shows that the observed slopes versus the magnetic field strength are much larger than those calculated assuming coupling into only the $\text{TE}_{1,1}$ mode. This results from emission into higher guide modes accessible to harmonics of the cyclotron frequency. Notably, as the β 's energies increase, the slopes align with the expectation based on radiation in free space. This can be intuitively understood given the significant increase in harmonic content of the radiation with field coupling to these higher modes. The calculation shown in Fig. 6 as a blue band confirms this expectation.

These two novel observations (long track segments and steep slopes) are important in optimizing data acquisition and analysis parameters as we move to accurate determinations of β spectra. The analysis of events must correctly identify start frequencies for short, low-slope tracks from $^{83\text{m}}\text{Kr}$ decays, and the long, sometimes non-linear, high-slope tracks associated with the higher-energy β s of ^6He and ^{19}Ne . The long tracks have an additional difficulty: variations in RF noise and gain versus frequency can lead to segmented tracks. All these issues were successfully addressed using an algorithm to cluster co-linear track segments.

Our present event rate for $^6\text{He}/^{19}\text{Ne}$ satisfying analysis cuts is only a few counts per second. A decay cell with thinner walls to reduce eddy currents and improved transmission of radioactivity are expected to increase observation rates to approximately 100 cps. Presently only about 10% of trapped β s have signals above the RF noise. Due to axial oscillations, which induce frequency modulation via the Doppler effect, power is diverted from the main band into sidebands [25]. About 90% of the

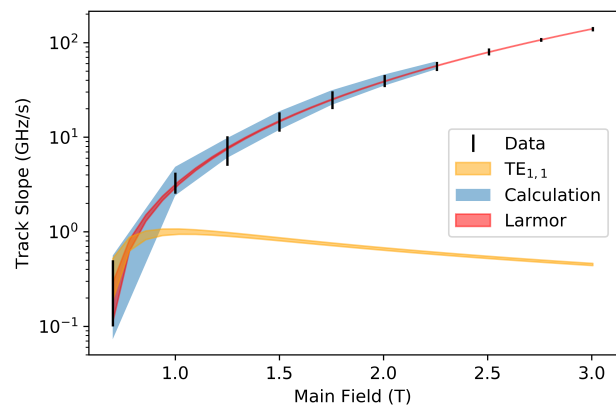


FIG. 6. Slopes, df/dt , versus field. Observed slopes (black lines) are much higher than expected from coupling only to the $\text{TE}_{1,1}$ mode (yellow band.) The blue band shows a calculation including coupling to 200 harmonics and 320,000 modes, presently limited by computing times. The red band is from the Larmor formula.

trapped electrons have oscillations with frequency modulation such that they are not observable with the present noise level. In principle, these effects can be accurately taken into account because they deterministically follow from the trap field and the β 's kinematic parameters. In addition, the product of the time series signals coming from both ends could eliminate sidebands, yielding a strong signal at twice the cyclotron frequency, but further developments in data acquisition and software are needed to implement these strategies.

A potential source of uncertainties for β spectra measured with this system is the “wall effect”. Although the magnetic trapping efficiency is independent of the magnitude of the momentum, the guide walls and the correlation between momentum and cyclotron radii result in smaller trappable volumes for β s with higher momenta. Any β that hits the wall quickly disappears. One can correct for this effect, but to reach beyond 10^{-3} accuracy in the spectrum would require knowledge of the radius to better than 10 microns and control of the cell-field misalignments at the part-per-thousand level. However, an analysis based on the ratio of ^6He and ^{19}Ne spectra allows for cancellation of this effect to first order, so the present demonstration of detection of signals from both ^6He and ^{19}Ne is an important milestone toward sensitive searches for non-zero Fierz interference effects.

An upgrade to the system is being investigated where ions would be injected instead of neutral atoms and the decay cell would become a Penning trap. With ions confined to the central axis of the trap-waveguide, the radial range of β s would be restricted, greatly diminishing the magnitude of the wall effect. Additionally, this development in connection with a facility such as FRIB would allow determination of spectra across a wide range of nuclei.

In summary, we presented the first observation of

CRES events for β s from ${}^6\text{He}$ and ${}^{19}\text{Ne}$ decays. Using a broad RF bandwidth and scanning the magnetic field, our apparatus can measure β s with kinetic energies in the 5 keV-to-5 MeV range. The radiation power emitted by β s in the waveguide was shown to present wide variations, according to the field, but this and other effects can be controlled for precision spectral measurements via the use of a combination of β^+ and β^- emitters. This Letter, therefore defines an important benchmark for the practical application of the CRES technique to a variety of nuclei covering the range of typical decay energies. This capability enables high precision determinations of β spectra that can be used to search for signatures of beyond-the-Standard-Model physics above the 1 TeV scale.

ACKNOWLEDGMENTS

We thank Andre Young, Christine Claessens, Ali Esfahani for useful guidance and discussions and David Peterson, Tim Van Wechel, and Ryan Roehnel for help with the apparatus. This work is supported by the US Department of Energy (DOE), Office of Nuclear Physics, under Contracts No. DE-AC02-06CH11357, DE-FG02-97ER41020, DE-FG02-ER41042, DE-AC05-76RL01830, DE-FG02-93ER40773, by the National Nuclear Security Administration under Award No. DE-NA0003841, by the National Science Foundation, grants No. NSF-1914133 and PHY-2012395, by the Gordon and Betty Moore Foundation and by the Cluster of Excellence ‘‘Precision Physics, Fundamental Interactions, and Structure of Matter’’ (PRISMA+ EXC 2118/1) funded by the German Research Foundation (DFG) within the German Excellence Strategy (Project ID 39083149). The ${}^{83}\text{Rb}$ – ${}^{83}\text{Kr}$ source used in this research was supplied by the DOE by the Isotope Program in the Office of Nuclear Physics.

-
- [1] V. Cirigliano, S. Gardner, and B. R. Holstein, Beta decays and non-standard interactions in the LHC era, *Progress in Particle and Nuclear Physics* **71**, 93 (2013).
- [2] M. Gonzalez-Alonso, O. Naviliat-Cuncic, and N. Severijns, New physics searches in nuclear and neutron β decay, *Progress in Particle and Nuclear Physics* **104**, 165 (2019).
- [3] T. Bhattacharya, V. Cirigliano, S. D. Cohen, A. Filipuzzi, M. González-Alonso, M. L. Graesser, R. Gupta, and H.-W. Lin, Probing novel scalar and tensor interactions from (ultra)cold neutrons to the LHC, *Physical Review D* **85**, 054512 (2012), [arXiv:1110.6448](https://arxiv.org/abs/1110.6448).
- [4] A. Falkowski, M. González-Alonso, and O. Naviliat-Cuncic, Comprehensive analysis of beta decays within and beyond the Standard Model, *Journal of High Energy Physics* **2021**, 126 (2021), [arXiv:2010.13797](https://arxiv.org/abs/2010.13797).
- [5] V. Cirigliano, D. Díaz-Calderón, A. Falkowski, M. González-Alonso, and A. Rodríguez-Sánchez, Semileptonic tau decays beyond the Standard Model, *Journal of High Energy Physics* **2022**, 152 (2022), [arXiv:2112.02087](https://arxiv.org/abs/2112.02087).
- [6] X. Sun, E. Adamek, B. Allgeier, Y. Bagdasarova, D. B. Berguno, M. Blatnik, T. J. Bowles, L. J. Broussard, M. A.-P. Brown, R. Carr, S. Clayton, C. Cude-Woods, S. Currie, E. B. Dees, X. Ding, B. W. Filippone, A. García, P. Geltenbort, S. Hasan, K. P. Hickerson, J. Hoagland, R. Hong, A. T. Holley, T. M. Ito, A. Knecht, C.-Y. Liu, J. Liu, M. Makela, R. Mammei, J. W. Martin, D. Melconian, M. P. Mendenhall, S. D. Moore, C. L. Morris, S. Nepal, N. Nouri, R. W. Pattie, A. Pérez Gálvan, D. G. Phillips, R. Picker, M. L. Pitt, B. Plaster, D. J. Salvat, A. Saunders, E. I. Sharapov, S. Sjue, S. Slutsky, W. Sondheim, C. Swank, E. Tatar, R. B. Vogelaar, B. VornDick, Z. Wang, W. Wei, J. W. Wexler, T. Womack, C. Wrede, A. R. Young, and B. A. Zeck (‘‘UCNA’’ Collaboration), Improved limits on Fierz interference using asymmetry measurements from the Ultracold Neutron Asymmetry (UCNA) experiment, *Phys. Rev. C* **101**, 035503 (2020).
- [7] H. Saul, C. Roick, H. Abele, H. Mest, M. Klopff, A. K. Petukhov, T. Soldner, X. Wang, D. Werder, and B. Märkisch, Limit on the Fierz Interference Term b from a Measurement of the Beta Asymmetry in Neutron Decay, *Phys. Rev. Lett.* **125**, 112501 (2020).
- [8] D. Počanić, R. Alarcon, L. Alonzi, S. Baeßler, S. Balascuta, J. Bowman, M. Bychkov, J. Byrne, J. Calarco, V. Cianciolo, C. Crawford, E. Frlež, M. Gericke, G. Greene, R. Grzywacz, V. Gudkov, F. Hersman, A. Klein, J. Martin, S. Page, A. Palladino, S. Penttilä, K. Rykaczewski, W. Wilburn, A. Young, and G. Young, Nab: Measurement principles, apparatus and uncertainties, *Nuclear Instruments and Methods in Physics Research Section A: Accelerators, Spectrometers, Detectors and Associated Equipment* **611**, 211 (2009), particle Physics with Slow Neutrons.
- [9] Fry, J., Alarcon, R., Baeßler, S., Balascuta, S., Palos, L. Barrón, Bailey, T., Bass, K., Birge, N., Blose, A., Borisenko, D., Bowman, J.D., Broussard, L.J., Bryant, A.T., Byrne, J., Calarco, J.R., Caylor, J., Chang, K., Chupp, T., Cianciolo, T.V., Crawford, C., Ding, X., Doyle, M., Fan, W., Farrar, W., Fomin, N., Frlez, E., Gericke, M.T., Gervais, M., Glück, F., Greene, G.L., Grzywacz, R.K., Gudkov, V., Hamblen, J., Hayes, C., Hendrus, C., Ito, T., Jezghani, A., Li, H., Makela, M., Macsai, N., Mammei, J., Mammei, R., Martinez, M., Matthews, D.G., McCreia, M., McGaughey, P., McLaughlin, C.D., Mueller, P., Petten, D. van, Penttilä, S.I., Perryman, D.E., Picker, R., Pierce, J., Pocanić, D., Qian, Y., Ramsey, J., Randall, G., Riley, G., Rykaczewski, K.P., Salas-Bacci, A., Samiei, S., Scott, E.M., Shelton, T., Sjue, S.K., Smith, A., Smith, E., Stevens, E., Wexler, J., Whitehead, R., Wilburn, W.S., Young, A., and Zeck, B., The Nab experiment: A precision measurement of unpolarized neutron beta decay, *EPJ Web Conf.* **219**, 04002 (2019).

- [10] D. Moser, H. Abele, J. Bosina, H. Fillunger, T. Soldner, X. Wang, J. Zmeskal, and G. Konrad, NoMoS: An $R \times B$ drift momentum spectrometer for beta decay studies, *EPJ Web Conf.* **219**, 04003 (2019).
- [11] X. Wang, C. Ziener, H. Abele, S. Bodmaier, D. Dubbers, J. Erhart, A. Hollering, E. Jericha, J. Klenke, H. Fillunger, W. Heil, C. Klauser, G. Konrad, M. Lamparth, T. Lauer, M. Klopff, R. Maix, B. Märkisch, W. Mach, H. Mest, D. Moser, A. Pethoukov, L. Raffelt, N. Rebroya, C. Roick, H. Saul, U. Schmidt, T. Soldner, R. Viro, O. Zimmer, and (the PERC collaboration), Design of the magnet system of the neutron decay facility PERC, *EPJ Web Conf.* **219**, 04007 (2019).
- [12] X. Huyan, O. Naviliat-Cuncic, P. Voytas, S. Chandavar, M. Hughes, K. Minamisono, and S. Paulauskas, Geant4 simulations of the absorption of photons in CsI and NaI produced by electrons with energies up to 4 MeV and their application to precision measurements of the β -energy spectrum with a calorimetric technique, *Nuclear Instruments and Methods in Physics Research Section A: Accelerators, Spectrometers, Detectors and Associated Equipment* **879**, 134 (2018).
- [13] X. Flechard, personal communication (2020).
- [14] A. Gorelov, D. Melconian, W. P. Alford, D. Ashery, G. Ball, J. A. Behr, P. G. Bricault, J. M. D'Auria, J. Deutsch, J. Dilling, M. Domsbky, P. Dubé, J. Fingler, U. Giesen, F. Glück, S. Gu, O. Häusser, K. P. Jackson, B. K. Jennings, M. R. Pearson, T. J. Stocki, T. B. Swanson, and M. Trinczek, Scalar Interaction Limits from the β - ν Correlation of Trapped Radioactive Atoms, *Phys. Rev. Lett.* **94**, 142501 (2005).
- [15] M. T. Burkey, G. Savard, A. T. Gallant, N. D. Scielzo, J. A. Clark, T. Y. Hirsh, L. Varriano, G. H. Sargsyan, K. D. Launey, M. Brodeur, D. P. Burdette, E. Heckmaier, K. Joerres, J. W. Klimes, K. Kolos, A. Laminack, K. G. Leach, A. F. Levand, B. Longfellow, B. Maaß, S. T. Marley, G. E. Morgan, P. Mueller, R. Orford, S. W. Padgett, A. Pérez Galván, J. R. Pierce, D. Ray, R. Segel, K. Siegl, K. S. Sharma, and B. S. Wang, Improved Limit on Tensor Currents in the Weak Interaction from ^8Li β Decay, *Phys. Rev. Lett.* **128**, 202502 (2022).
- [16] P. Alfauert *et al.*, WISArD : Weak Interaction Studies with ^{32}Ar Decay, *PoS PANIC2021*, 449 (2022).
- [17] B. Fenker, A. Gorelov, D. Melconian, J. A. Behr, M. Anholm, D. Ashery, R. S. Behling, I. Cohen, I. Craiciu, G. Gwinner, J. McNeil, M. Mehlman, K. Olchanski, P. D. Shidling, S. Smale, and C. L. Warner, Precision Measurement of the β Asymmetry in Spin-Polarized ^{37}K Decay, *Phys. Rev. Lett.* **120**, 062502 (2018).
- [18] L. D. Knutson, G. W. Severin, S. L. Cotter, L. Zhan, P. A. Voytas, and E. A. George, A superconducting beta spectrometer, *Review of Scientific Instruments* **82**, 073302 (2011), <https://doi.org/10.1063/1.3608454>.
- [19] P. O'Malley, M. Brodeur, D. Burdette, J. Klimes, A. Valverde, J. Clark, G. Savard, R. Ringle, and V. Varentsov, Testing the weak interaction using St. Benedict at the University of Notre Dame, *Nuclear Instruments and Methods in Physics Research Section B: Beam Interactions with Materials and Atoms* **463**, 488 (2020).
- [20] P. Shidling, M. Mehlman, V. Kolhinen, G. Chubarian, L. Cooper, G. Duran, E. Gilg, V. Iacob, K. Marble, R. McAfee, D. McClain, M. McDonough, M. Nasser, C. Gonzalez-Ortiz, A. Ozmetin, B. Schroeder, M. Soulard, G. Tabacaru, and D. Melconian, The TAMU-TRAP facility: A Penning trap facility at Texas A&M University for weak interaction studies, *International Journal of Mass Spectrometry* **468**, 116636 (2021).
- [21] E. A. George, P. A. Voytas, G. W. Severin, and L. D. Knutson, Measurement of the shape factor for the β decay of ^{14}O , *Phys. Rev. C* **90**, 065501 (2014).
- [22] P. A. Voytas, E. A. George, G. W. Severin, L. Zhan, and L. D. Knutson, Measurement of the branching ratio for the β decay of ^{14}O , *Phys. Rev. C* **92**, 065502 (2015).
- [23] B. Monreal and J. A. Formaggio, Relativistic cyclotron radiation detection of tritium decay electrons as a new technique for measuring the neutrino mass, *Phys. Rev. D* **80**, 051301 (2009).
- [24] D. M. Asner, R. F. Bradley, L. de Viveiros, P. J. Doe, J. L. Fernandes, M. Fertl, E. C. Finn, J. A. Formaggio, D. Furse, A. M. Jones, J. N. Kofron, B. H. LaRoque, M. Leber, E. L. McBride, M. L. Miller, P. Mohanmurthy, B. Monreal, N. S. Oblath, R. G. H. Robertson, L. J. Rosenberg, G. Rybka, D. Rysewyk, M. G. Sternberg, J. R. Tedeschi, T. Thümmeler, B. A. VanDevender, and N. L. Woods (Project 8 Collaboration), Single-electron detection and spectroscopy via relativistic cyclotron radiation, *Phys. Rev. Lett.* **114**, 162501 (2015).
- [25] A. A. Esfahani, V. Bansal, S. Böser, N. Buzinsky, R. Cervantes, C. Claessens, L. de Viveiros, P. J. Doe, M. Fertl, J. A. Formaggio, L. Gladstone, M. Guigue, K. M. Heeger, J. Johnston, A. M. Jones, K. Kazkaz, B. H. LaRoque, M. Leber, A. Lindman, E. Machado, B. Monreal, E. C. Morrison, J. A. Nikkel, E. Novitski, N. S. Oblath, W. Petrus, R. G. H. Robertson, G. Rybka, L. Saldaña, V. Sibille, M. Schram, P. L. Slocum, Y.-H. Sun, J. R. Tedeschi, T. Thümmeler, B. A. VanDevender, M. Wachtendonk, M. Walter, T. E. Weiss, T. Wendler, and E. Zayas (Project 8 Collaboration), Electron radiated power in cyclotron radiation emission spectroscopy experiments, *Phys. Rev. C* **99**, 055501 (2019).
- [26] O. Naviliat-Cuncic and N. Severijns, Test of the Conserved Vector Current Hypothesis in $T = 1/2$ Mirror Transitions and New Determination of $|V_{ud}|$, *Phys. Rev. Lett.* **102**, 142302 (2009).
- [27] A. Knecht, R. Hong, D. W. Zumwalt, B. G. Delbridge, A. García, P. Müller, H. E. Swanson, I. S. Towner, S. Utsuno, W. Williams, and C. Wrede, Precision Measurement of the ^6He Half-Life and the Weak Axial Current in Nuclei, *Phys. Rev. Lett.* **108**, 122502 (2012).
- [28] D. Combs, G. Jones, W. Anderson, F. Calaprice, L. Hayen, and A. Young, *A look into mirrors: A measurement of the β -asymmetry in ^{19}Ne decay and searches for new physics* (2020).
- [29] P. Müller, Y. Bagdasarova, R. Hong, A. Leredde, K. G. Bailey, X. Fléchar, A. García, B. Graner, A. Knecht, O. Naviliat-Cuncic, T. O'Connor, M. Sternberg, D. Storm, H. E. Swanson, F. Wauters, and D. Zumwalt, β -nuclear-recoil correlation from ^6He decay in a laser trap, *Phys. Rev. Lett.* (2022), in press.
- [30] J. D. Jackson, S. B. Treiman, and H. W. Wyld, Possible tests of time reversal invariance in beta decay, *Phys. Rev.* **106**, 517 (1957).
- [31] A. Knecht, D. Zumwalt, B. Delbridge, A. García, G. Harper, R. Hong, P. Müller, A. Palmer, R. Robertson, H. Swanson, S. Utsuno, D. Will, W. Williams, and C. Wrede, A high-intensity source of ^6He atoms for fundamental research, *Nuclear Instruments and Methods in Physics Research Section A: Accelerators, Spectrometers,*

- Detectors and Associated Equipment** **660**, 43 (2011).
- [32] D. Dobson, *The beta-decay asymmetry and nuclear magnetic moment of Neon-19*, **Ph.D. thesis**, University of California, Berkeley (1963).
- [33] D. Girvin, *Test of time-reversal invariance in ^{19}Ne beta decay*, Ph.D. thesis, University of California, Berkeley (1972).
- [34] F. P. Calaprice, E. D. Commins, and D. C. Girvin, New test of time-reversal invariance in ^{19}Ne beta decay, **Phys. Rev. D** **9**, 519 (1974).
- [35] M. B. Schneider, F. P. Calaprice, A. L. Hallin, D. W. MacArthur, and D. F. Schreiber, Limit on $\text{Im}(C_S C_A^*)$ from a Test of T Invariance in ^{19}Ne Beta Decay, **Phys. Rev. Lett.** **51**, 1239 (1983).
- [36] D. Vénos, A. Špalek, O. Lebeda, and M. Fišer, ^{83m}Kr radioactive source based on ^{83}Rb trapped in cation-exchange paper or in zeolite, **Applied Radiation and Isotopes** **63**, 323 (2005).
- [37] <https://lownoisefactory.com/> (2022), LNAs were LNF – LNC16 – 28WB from Low Noise Factory.
- [38] P8 (Project 8 Collaboration), Private communication (2022).
- [39] Casper (Casper Collaboration), CASPER, ROACH2 system, <https://casper.astro.berkeley.edu/wiki/ROACH2> (2013).
- [40] N. S. Oblath, N. Buzinsky, C. Claessens, L. Gladstone, M. Guigue, J. Huang, B. Johnson, J. Kofron, B. LaRoque, E. Novitski, D. Rysewyk, L. Saldaña, P. Slocum, Y.-H. Sun, B. VanDevender, L. de Viveiros, and E. Zayas, **Katydid: Project 8 analysis software package**, <https://doi.org/10.5281/zenodo.2621293>[doi.org] (2019).
- [41] J. D. Jackson, *Classical Electrodynamics*, 3rd ed. (John Wiley & Sons, Inc., New Jersey, USA, 1991).
- [42] D. M. Pozar, *Microwave engineering; 3rd ed.* (Wiley, Hoboken, NJ, 2005).
- [43] D. Kleppner, Inhibited Spontaneous Emission, **Phys. Rev. Lett.** **47**, 233 (1981).